



Cite this: *Phys. Chem. Chem. Phys.*,
2015, 17, 2335

Received 15th October 2014,
Accepted 4th December 2014

DOI: 10.1039/c4cp04685d

www.rsc.org/pccp

Hole-transport materials with greatly-differing redox potentials give efficient TiO_2 - $[\text{CH}_3\text{NH}_3][\text{PbX}_3]$ perovskite solar cells†

Antonio Abate,^{‡a} Miquel Planells,^{‡b} Derek J. Hollman,^a Vishal Barthi,^c
Suresh Chand,^c Henry J. Snaith^{*a} and Neil Robertson^{*b}

Two diacetylide-triphenylamine hole-transport materials (HTM) with varying redox potential have been applied in planar junction TiO_2 - $[\text{CH}_3\text{NH}_3]\text{PbI}_{3-x}\text{Cl}_x$ solar cells leading to high power-conversion efficiencies up to 8.8%. More positive oxidation potential of the HTM gives higher V_{OC} and lower J_{SC} illustrating the role of matching energy levels, however both HTMs gave efficient cells despite a difference of 0.44 V in their redox potentials.

The recent development of lead halide perovskite based solar cells has led to a step change in the efficiencies of solution-processable solar cells culminating recently in certified power-conversion efficiencies reaching the range 16–18%.¹ The exceptional performance of these devices has been attributed to key properties of the perovskite layer including excellent electron and exciton mobility and direct band gap of appropriate energy for visible light harvesting.²

To date, **Spiro-OMeTAD** has been most commonly used as the HTM in the highest efficiency cells, however this material requires an expensive multi-step synthesis and shows hole-transport too low to carry all generated current.^{3,4} In response, there has been increased recent interest in developing new HTMs aimed at addressing these limitations.^{3–12} This work has explored alternative HTM structures, in particular based on the triarylamine and carbazole motifs,^{6–11} leading to impressive power-conversion efficiencies (PCE) reaching around 14%.⁶ In general however, these studies have paid limited attention

to the exact redox properties of the new HTM provided the value lay approximately close to **Spiro-OMeTAD**, despite the fact that this molecule was designed for OLEDs and employed in solid-state dye-sensitised solar cells (ssDSSC) rather than perovskite cells.

Our recent work has led to a new diacetylide-triphenylamine (DATPA) series of HTMs,¹³ prepared by a simple synthetic route, which in turn allows much easier tuning of electrochemical and other properties through varying the substituent R groups. These were studied as HTMs in ssDSSC and showed promising properties in comparison with **Spiro-OMeTAD**, with the key difference being the differing redox potentials. In this work, we now report a new dimethyl amino substituted HTM (**Me₂N-DATPA**) with very low first oxidation potential. We have used this, and our previously-reported (in the context of ssDSSC) **MeO-DATPA**, to prepare planar-junction TiO_2 - $[\text{CH}_3\text{NH}_3]\text{PbI}_{3-x}\text{Cl}_x$ solar cells, the first perovskite cells that use the DATPA HTM series. This represents the first study specifically showing the effect of varying redox potential of structurally-similar HTMs on cell performance parameters.

The new **Me₂N-DATPA** molecule (Fig. 1a) was synthesised by a similar route to that we already reported for **MeO-DATPA**.¹³ This involved Ullmann coupling to form the triarylamine fragment, followed by Sonogashira coupling to add a trimethylsilyl acetylide fragment and, after deprotection to remove the trimethylsilyl unit, a final oxidative homocoupling to form the central diacetylide unit (see ESI† for full details).

Single crystals suitable for X-ray diffraction (XRD) were obtained by layer addition in EtOAc/DMSO. **Me₂N-DATPA** crystallised in the space group $P2_1/n$ and showed one molecule in the asymmetric unit (ESI†). The structure is arranged with the central diacetylide moieties approximately parallel between molecules. As expected the geometry around each triphenylamine is approximately planar and viewed along the long molecular axis, the molecules form herringbone arrangements that run in alternating directions. No intermolecular interactions are within van der Waal radii, however the positioning of **Me₂N**- groups on the periphery of the molecule enables

^a Department of Physics, University of Oxford, Oxford, OX1 3PU, UK

^b EastChem School of Chemistry, Kings Buildings, University of Edinburgh, Edinburgh, EH9 3JJ, UK. E-mail: neil.robertson@ed.ac.uk

^c CSIR-National Physical Laboratory, Dr. K.S. Krishnan Marg, New Delhi-110012, India

† Electronic supplementary information (ESI) available: Synthesis of **Me₂N-DATPA**; details of characterisation methods and solar cell fabrication. Figures: cyclic and square-wave voltammeteries, UV-Visible absorption and photoluminescence spectra, packing diagram for **Me₂N-DATPA**, J - V data for SCLC hole mobility at different temperatures. Crystallographic table. CCDC 936124. For ESI and crystallographic data in CIF or other electronic format see DOI: 10.1039/c4cp04685d

‡ These authors contributed equally.

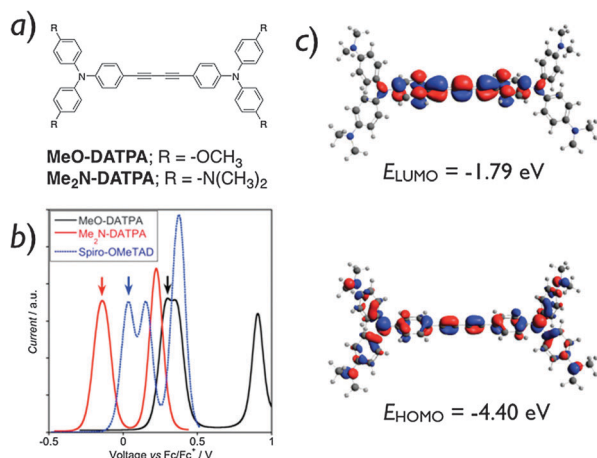


Fig. 1 (a) Molecular structure of DATPA derivatives used in this study; (b) square-wave voltammetry (SWV) traces of the HTMs referenced to ferrocene. The arrow indicates the first oxidation potential from which E_{HOMO} is derived and (c) molecular orbital distribution for **Me₂N-DATPA** at B3LYP/6-31G(d) level of theory (isodensity = 0.04). Absolute HOMO and LUMO energy values are experimentally obtained (see Table 1).

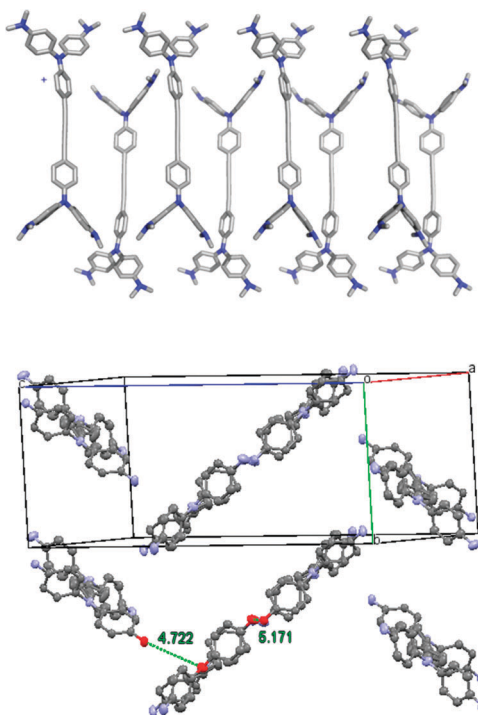


Fig. 2 Crystal structure of **Me₂N-DATPA** viewed along the short (upper) and long (lower) molecular axis. For clarity, methyl groups are removed in the lower view and short N...N contacts are indicated.

N...N contacts of 4.722 Å and 5.171 Å that link the molecules in a 2-D sheet (Fig. 2). Since the HOMO extends across the whole molecule including the peripheral nitrogen atoms (Fig. 1c) such contacts can enhance effective hole transport within the material.

To assess the essential energy levels of **Me₂N-DATPA**, electrochemical analysis (cyclic and square-wave voltammetry) were performed to obtain the HOMO energy level. Spectroscopic

Table 1 Summary of optical and electrochemical properties of HTM used in this study acquired in CH₂Cl₂ solution

HTM	λ_{max}^a / nm	λ_{em}^b / nm	E_{gap}^c / eV	E_{OX}^d / V	E_{HOMO}^e / eV	E_{LUMO}^f / eV
MeO-DATPA ^a	389	490	2.86	+0.30	−5.02	−2.29
Spiro-OMeTAD ^a	385	424	3.05	+0.03	−4.64	−2.16
Me₂N-DATPA	402	630	2.61	−0.14	−4.40	−1.79

^a Data from our previous work.¹³ ^b Excitation at λ_{max} . ^c From the intersection of absorption and emission spectra. ^d From SWV and CV measurements and referenced internally to ferrocene. ^e E_{HOMO} (eV) = $-1.4 E_{\text{OX}}$ (V) -4.6 . ^f $E_{\text{LUMO}} = E_{\text{HOMO}} + E_{\text{gap}}$.

methods (absorption and emission) were used to determine the gap and thus the LUMO energy level. Full details are given in ESI† and a summary of the resulting data given in Table 1 compared also with **Spiro-OMeTAD** and **MeO-DATPA**. Firstly, this confirmed little visible absorption by **Me₂N-DATPA**, in keeping with **MeO-DATPA** such that neither will significantly compete with the perovskite layer in the solar cell for light harvesting. The three HTMs differ markedly however in first oxidation potential, with that of **Me₂N-DATPA** being 0.44 V less positive than **MeO-DATPA** and 0.17 V less positive than **Spiro-**

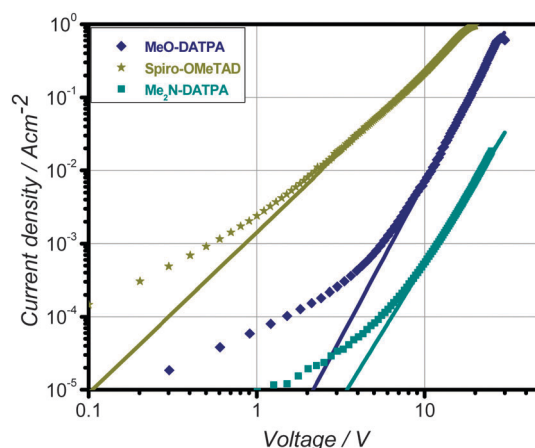


Fig. 3 J–V data for SCLC method of hole-mobility determination.

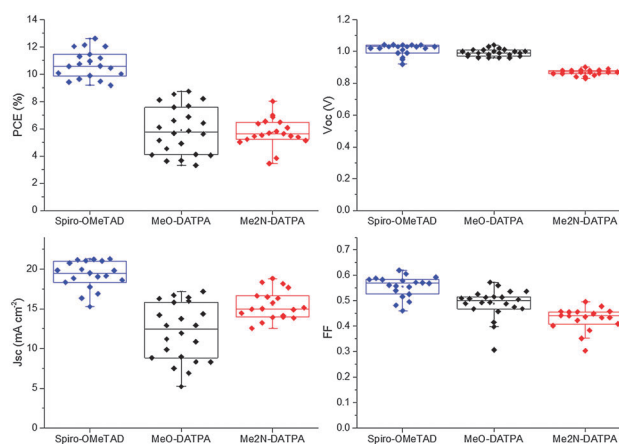


Fig. 4 Solar cell parameters over 20 repeats for each HTM.

Table 2 Summary of solar cell performance showing best and average PCE for each HTM, along with related parameters

HTM	V_{OC}/mV	$J_{SC}/\text{mA cm}^{-2}$	ff	PCE/%	$\mu/\text{cm}^2 \text{ V}^{-1} \text{ s}^{-1}$
Spiro-best	1.03	21.24	0.58	12.6	
Spiro-av	1.03 ± 0.03	19.52 ± 1.75	0.57 ± 0.04	10.6 ± 1.0	3.6×10^{-4}
MeO-best	0.96	16.41	0.56	8.8	
MeO-av	0.99 ± 0.02	12.40 ± 3.64	0.50 ± 0.06	5.9 ± 1.7	6.0×10^{-6}
Me ₂ N-best	0.87	18.80	0.50	8.0	
Me ₂ N-av	0.87 ± 0.02	14.99 ± 1.82	0.44 ± 0.04	5.7 ± 1.1	1.2×10^{-5}

OMeTAD (Fig. 1b). This makes the new **Me₂N-DATPA** HTM a significantly stronger donor molecule (*i.e.* stronger hole acceptor) than either of the other two HTMs used to prepare the solar cells.

These observations were generally reinforced by calculations at the B3LYP/6-31G(d) level of theory with C-PCM in CH₂Cl₂, which showed a difference in HOMO energy levels of around 0.3 eV between **Me₂N-** and **MeO-DATPA**. The delocalisation of the HOMO onto the peripheral substituents (Fig. 1c) explains the large shift in oxidation potential upon changing from MeO- to Me₂N-, and also favours the strong interactions between HOMOs of adjacent molecules required for effective hole transport.

To assess the hole-transport properties, a space-charge limited current (SCLC) method was used according to the methodology reported in detail in ESI† (Fig. 3 and Fig. S4).¹³ This involved a spin-coated layer of the HTM on an ITO/PEDOT-PSS substrate, followed by an evaporated gold counter electrode. Since the ITO and gold work functions are close to the HTM HOMO level, this creates a hole-only device from which the mobility can be determined. This led to a room-temperature value of $1.2 \times 10^{-5} \text{ cm}^2 \text{ V}^{-1} \text{ s}^{-1}$ for **Me₂N-DATPA** and lower values at reduced temperature, in keeping with a thermally-activated process. In comparison with our previously-reported value of $6.0 \times 10^{-6} \text{ cm}^2 \text{ V}^{-1} \text{ s}^{-1}$ for **MeO-DATPA** under the same conditions, the slightly higher mobility for the new HTM may arise from N...N interactions involving the peripheral Me₂N groups of the former as shown in Fig. 2. Overall however, the two values differ by only a factor of two and it seems likely that the significantly altered redox potential will play a larger role in solar cell performance.

We prepared perovskite solar cells in keeping with previously reported methods and as described in detail in ESI†. DATPA derivatives and **Spiro-OMeTAD** were doped with protic ionic liquids following the method similar to that previously published¹⁵ and as described more in detail in ESI†. All cells were prepared in a single continuous study using identical methods over 20 repeat cells for each HTM, enabling reliable comparison between the DATPA HTMs and **Spiro-OMeTAD** (Fig. 4 and Table 2). The latter showed the highest power-conversion efficiency (PCE) of 12.6%, however the corresponding values of 8.8% and 8.0% for **MeO-** and **Me₂N-DATPA** respectively are remarkably high for the first studies of new HTMs, given that **Spiro-OMeTAD** has undergone extensive optimisation of the doping and processing procedures over many years.

Although the overall PCEs for the DATPA HTMs are similar, consideration of their V_{OC} and J_{SC} values reveals different origins to their respective performance. The average J_{SC} is increased by 2.5 mA cm^{-2} in changing from the weaker electron donor

MeO-DATPA to the stronger **Me₂N-DATPA** indicating that the ability of the hole to be transferred efficiently to the HTM plays a crucial role in these cells. On the other hand, the HOMO level of **Me₂N-DATPA** is closer to vacuum, expected to lead to a smaller splitting of the quasi Fermi levels upon illumination between the TiO₂ and the HTM and this leads to the smaller V_{OC} for the latter.

We have prepared a new hole-transport material with a very strong hole-donor capability, adding to the redox-tunable series of substituted-DATPA HTMs we reported previously in the context of ssDSSC.¹³ For the first time we have applied two DATPA molecules as the HTMs in perovskite solar cells leading to excellent efficiencies in both cases, despite the large difference in hole-donor strength. Close inspection indicates a trade-off in V_{OC} with J_{SC} as the HTM redox potential is changed, however the differences are perhaps not as great as might be expected; a 0.44 V difference in oxidation potential between the DATPA HTMs leads to only a 0.12 V difference in average V_{OC} of the resulting cells. Likewise a difference in average J_{SC} of only 2.5 mA cm^{-2} is observed despite the 0.44 V difference in driving force for hole transfer. In contrast with solid or liquid-electrolyte dye-sensitised solar cells, this implies a wide tolerance of perovskite solar cells to function well with HTMs of greatly differing redox potential, suggesting a wider palette of HTMs might be explored for the further development of these devices.

Acknowledgements

We thank the EPSRC (APEX Project, EP/H040218/1) for financial support. We thank Dr Gary Nichol, University of Edinburgh for the crystallographic data collection and refinement and the EaStCHEM computational facility for access.

Notes and references

- 1 H. Zhou, Q. Chen, G. Li, S. Luo, T.-B. Song, H.-S. Duan, Z. Hong, J. You, Y. Liu and Y. Yang, *Science*, 2014, **345**, 542; N. J. Jeon, J. H. Noh, Y. C. Kim, W. S. Yang, S. Ryu and S. I. Seok, *Nat. Mater.*, 2014, **13**, 897.
- 2 M. Grätzel, *Nat. Mater.*, 2014, **13**, 838.
- 3 B. Xu, E. Sheibani, P. Liu, J. Zhang, H. Tian, N. Vlachopoulos, G. Boschloo, L. Kloo, A. Hagfeldt and L. Sun, *Adv. Mater.*, 2014, **26**, 6629.
- 4 H. Zhang, Y. Shi, F. Yan, L. Wang, K. Wang, Y. Xing, Q. Dong and T. Ma, *Chem. Commun.*, 2014, **50**, 5020.
- 5 H. Choi, S. Paek, N. Lim, Y. H. Lee, M. K. Nazeeruddin and J. Ko, *Chem. – Eur. J.*, 2014, **20**, 10894.

- 6 H. Li, K. Fu, A. Hagfeldt, M. Grätzel, S. G. Mhaisalkar and A. C. Grimsdale, *Angew. Chem., Int. Ed.*, 2014, **53**, 4085.
- 7 T. Krishnamoorthy, F. Kunwu, P. P. Box, H. Li, T. M. Koh, W. L. Leong, S. Powar, A. Grimsdale, M. Grätzel, N. Mathews and S. G. Mhaisalkar, *J. Mater. Chem. A*, 2014, **2**, 6305.
- 8 J. Wang, S. Wang, X. Li, L. Zhu, Q. Meng, Y. Xiao and D. Li, *Chem. Commun.*, 2014, **50**, 5829.
- 9 D. Bi, L. Yang, G. Boschloo, A. Hagfeldt and E. M. J. Johansson, *J. Phys. Chem. Lett.*, 2013, **4**, 1532.
- 10 S. Lv, L. Han, J. Xiao, L. Zhu, J. Shi, H. Wei, Y. Xu, J. Dong, X. Xu, D. Li, S. Wang, Y. Luo, Q. Meng and X. Li, *Chem. Commun.*, 2014, **50**, 6931.
- 11 P. Qin, S. Paek, M. I. Dar, N. Pellet, J. Ko, M. Grätzel and M. K. Nazeeruddin, *J. Am. Chem. Soc.*, 2014, **136**, 8516.
- 12 K. Do, H. Choi, K. Lim, H. Jo, J. W. Cho, M. K. Nazeeruddin and J. Ko, *Chem. Commun.*, 2014, **50**, 10971.
- 13 M. Planells, A. Abate, D. J. Hollman, S. D. Stranks, V. Bharti, J. Gaur, D. Mohanty, S. Chand, H. J. Snaith and N. Robertson, *J. Mater. Chem. A*, 2013, **1**, 6949.
- 14 B. W. D'Andrade, S. Datta, S. R. Forrest, P. Djurovich, E. Polikarpov and M. E. Thompson, *Org. Electron.*, 2005, **6**, 11.
- 15 A. Abate, D. J. Hollman, J. Teuscher, S. Pathak, R. Avolio, G. D'Errico, G. Vitiello, S. Fantacci and H. J. Snaith, *J. Am. Chem. Soc.*, 2013, **135**, 13538.